

# Detection of Native Amino Acids and Peptides Utilizing Sinusoidal Voltammetry

Sara A. Brazill,<sup>†</sup> Pankaj Singhal,<sup>‡</sup> and Werner G. Kuhr<sup>\*,†</sup>

Department of Chemistry, University of California, Riverside, California 92521-0403, and Clinical Microsensors, 126 West Del Mar Boulevard, Pasadena, California 91105

**Native amino acids and peptides were detected at a copper microelectrode using sinusoidal voltammetry (SV). Traditionally, these molecules can only be measured after derivatization with either a fluorescent or electroactive tag. In this work, an electrocatalytic oxidation reaction at copper is used to detect underivatized peptides and amino acids. The oxidation reaction is somewhat independent of peptide structure (i.e., it is not limited to the detection of aromatic amino acids) and is therefore able to produce nanomolar detection limits for all amino acids and peptides tested. A scanning technique, sinusoidal voltammetry, is used to provide the sensitivity of constant-potential techniques but also provide selectivity gained through utilization of the frequency domain. The frequency spectrum due to the oxidation of each molecule has a unique “fingerprint” response resulting from the kinetics of oxidation at the electrode surface. Through examination of the frequency spectra, even structurally similar molecules can be easily distinguished from one another. Flow injection analysis is used to demonstrate the sensitive and selective detection of a variety of amino acids and peptides. This technique can also be easily coupled to a separation step, i.e., high-performance liquid chromatography or capillary electrophoresis without electrode fouling from the adsorption of the analytes.**

Amino acids and neuroactive peptides are important biological molecules and play key roles in many neurochemical response mechanisms, such as memory, appetite control, and pain transmission.<sup>1–4</sup> The disruption of their regulation has also been linked to many disorders such as Huntington's, Alzheimer's, and Parkinson's diseases.<sup>2,4,5</sup> The development of a simple and universal detection method for these compounds would help us to better understand their biological role and facilitate the design of drugs to combat these diseases. The ability to detect amino acids, peptides, and proteins in their native state is highly desirable

in order to avoid time- and labor-intensive derivatization steps and minimize sample handling, which is plagued with contamination and dilution problems.

There has been a great deal of work in the development of detection strategies for amino acids and peptides, whose analysis is almost always coupled to a separation step (e.g., chromatography or electrophoresis) before detection. Therefore, the detection method must be both mass and concentration sensitive to be able to detect the small amount of analyte eluting during the separation. While a commonly used detection method for amino acids and peptides is UV absorbance, it is inappropriate for use with capillary separation methods because it is concentration insensitive ( $\mu\text{M}$  range) due to the low absorptivity of most amino acids and the path length dependence of the detection limit.<sup>6</sup> Fluorescence detection has been used as an alternative in the detection of amino acids and peptides. The native fluorescence of tryptophan and tyrosine in the 210–290 nm range has been demonstrated to be a sensitive method with high-picomolar to low-nanomolar limits of detection (LOD).<sup>7</sup> However, not all peptides contain either of these amino acids and other native amino acids cannot be detected by this method. To overcome this limitation, the amino acids and peptides can be derivatized with a fluorescent molecule and then detected with laser-induced fluorescence (LIF).

LIF is a sensitive technique with reported detection limits for derivatized peptides in the low-picomolar (attomole) range.<sup>2,3,8–10</sup> Some of the compounds used for derivatization include naphthalene-2,3-dicarboxaldehyde (NDA),<sup>2,10</sup> o-phthalaldehyde (OPA),<sup>9</sup> fluorescein isothiocyanate (FITC),<sup>3</sup> and 3-(4-carboxybenzoyl)2-quinolinecarboxaldehyde (CBQCA),<sup>8</sup> which react with primary and secondary amines. One problem with this derivatization scheme is that peptides without reactive amines such as cyclic peptides, N-acylated peptides, and peptides with pyroglutamate at the amine terminus are not readily derivatized.<sup>11,12</sup> Other possible complications include multiple tagging of lysine-containing peptides and

\* To whom correspondence should be addressed: (e-mail) Werner.Kuhr@ucr.edu.

<sup>†</sup> University of California.

<sup>‡</sup> Clinical Microsensors.

(1) Hokfelt, T. *Neuron* **1991**, *7*, 867–879.

(2) Kostel, K. L.; Lunte, S. M. *J. Chromatogr., B* **1997**, *695*, 27–38.

(3) Toulas, C.; Hernandez, L. *Analisis* **1992**, *20*, 583–585.

(4) Shen, H.; Witowski, S. R.; Boyd, B. W.; Kennedy, R. T. *Anal. Chem.* **1999**, *71*, 987–994.

(5) Boyd, B. W.; Witowski, S. R.; Kennedy, R. T. *Anal. Chem.* **2000**, *72*, 865–871.

(6) Smith, J. T. *Electrophoresis* **1999**, *20*, 3078–3083.

(7) Timperman, A. T.; Oldenburg, K. E.; Sweedler, J. V. *Anal. Chem.* **1995**, *67*, 3421–3426.

(8) Bergquist, J.; Vona, M. J.; Stiller, C. O.; Oconnor, W. T.; Falkenberg, T.; Ekman, R. *J. Neurosci. Methods* **1996**, *65*, 33–42.

(9) Orwar, O.; Folestad, S.; Einarsson, S.; Andine, P.; Sandberg, M. *J. Chromatogr.-Biomed. Appl.* **1991**, *566*, 39–55.

(10) Oates, M. D.; Cooper, B. R.; Jorgenson, J. W. *Anal. Chem.* **1990**, *62*, 1573–1577.

(11) Chen, J. G.; Wolzman, S. J.; Weber, S. G. *J. Chromatogr., A* **1995**, *691*, 301–315.

(12) Warner, A. M.; Weber, S. G. *Anal. Chem.* **1989**, *61*, 2664–2668.

derivatization of other primary amines in the sample matrix, resulting in unwanted side products. Some of the derivatization starting materials are themselves fluorescent, and the excess reagent needed to ensure the derivatization reaction proceeds to completion needs to be removed before analysis.<sup>13</sup> Clearly, the need for a derivatization step is not ideal because of possible contamination and loss of the biological sample.

Several researchers have used electrochemical methods for the detection of amino acids and peptides.<sup>4,10</sup> At modest potentials, only tryptophan, tyrosine, and cysteine are electroactive at traditional carbon electrodes, while most amino acids are not easily oxidized.<sup>14–17</sup> Kennedy et al. have used carbon fiber electrodes to detect underderivatized tyrosine- and tryptophan-containing peptides.<sup>17,18</sup> They have shown that peptides such as, met-enkephalin and melanocyte stimulating hormone, can be detected in picomolar concentrations after on-column preconcentration. They also demonstrated the compatibility of electrochemical detection with microdialysis sampling *in vivo*. Although the native detection of electroactive peptides is a sensitive technique, it lacks the universal applicability desired. Derivatization with electroactive molecules can also be used to detect amino acids and peptides at carbon electrodes.<sup>5,19,20</sup> However, similar to derivation in LIF detection, it still requires an extra derivatization step, which is problematic for biological applications.

Others have used noble and catalytic metals as electrode materials for the detection of aliphatic compounds. The use of most noble metals, such as Au<sup>21,22</sup> and Pt,<sup>21,23</sup> is complicated by fouling of the electrode surface with oxidative products, which tend to irreversibly adsorb onto the electrode surface, blocking active electron-transfer sites. Therefore, due to the strong adsorption of most peptides onto these electrodes, dc amperometric detection is not usually possible. Pulsed amperometric detection (PAD, which uses a multistep waveform to detect, clean, and reactivate the electrode surface) has been used to alleviate the inactivation of the electrode surface.<sup>21–23</sup> However, since PAD uses a multistep waveform and discriminates against the background in the time domain, much of the signal intensity is lost. Attractive alternatives for the detection of amino acids and peptides are

electrocatalytic metals such as Cu<sup>24–30</sup> and Ni<sup>31</sup> or chemically modified carbon electrodes.<sup>30,32</sup>

Detection of amino acids at a copper electrode has been postulated to be due to either a complexation<sup>24–27</sup> or electrocatalytic<sup>28,29,32–35</sup> mechanism. The surface of the copper electrode is complex, believed to contain both soluble and insoluble layers. Ewing et al. and others have shown that a stable bilayer film forms on the Cu electrode surface at slightly positive potentials.<sup>26,27</sup> The first layer is reported to be a highly insoluble layer of copper(I) oxide that shields the Cu surface from direct contact with the analyte. The second layer is believed to contain a highly soluble layer of copper(II) oxide and cupric salts. Complexation with the Cu(II) ions results in the enhanced solubility of the outer layer and thus the increase in the steady-state current. Even though this method gives micromolar (femtomole) to high-nanomolar (attomole) detection limits, application to larger peptides and proteins is not straightforward. Another Cu(II) complexation reaction used to sensitively detect peptides is the biuret reaction. Weber et al., among others, have used the biuret reaction to electrochemically detect peptides at carbon electrodes.<sup>4,11,12,36,37</sup> The electrochemical signal for many peptides arises from the reversible Cu(II)–peptide Cu(III)–peptide redox couple at 0.7–0.9 V vs Ag/AgCl.<sup>38</sup> This method has been shown to be very sensitive with detection limits for many peptides including substance P, bradykinin, and neurotensin, in the low-picomolar range.<sup>4</sup> However, the biuret reaction cannot detect amino acids since they lack the amide linkage needed for complexation.

The second possible detection mechanism at a copper electrode, electrocatalytic oxidation, is believed to give the greatest sensitivity and applicability to larger molecules.<sup>28–30</sup> It has been proposed that a soluble layer of metal oxide or hydroxide forms (e.g., CuO(OH)) initially under alkaline conditions and that it is this species that behaves as a redox mediator for the catalytic oxidation at potentials greater than 0.4 V.<sup>28,32–35</sup> Baldwin et al. have used dc amperometry to detect native amino acids and peptides at a copper electrode with an electrocatalytic mechanism.<sup>28,30</sup> They achieved detection limits from 40 nM to 2  $\mu$ M for most native amino acids and small peptides.

Previous work in this laboratory has utilized sinusoidal voltammetry (SV) to detect unlabeled carbohydrates,<sup>39</sup> nucleotides,<sup>40</sup> ss-DNA, and ds-DNA<sup>41,42</sup> at a copper electrode. A sine wave is used as the excitation waveform to sweep through the entire potential region of interest. The resulting current response is nonlinear, with signal component at the fundamental harmonic as well as higher order harmonics. However, the major background component, which is typically the charging current associated with the electrochemical double layer, is primarily linear with a major component at the fundamental frequency.

---

(13) Sherwood, R. *J. Neurosci. Methods* **1990**, *34*, 17–22.  
 (14) Fleming, L.; Reynolds, N. *J. Chromatogr.* **1986**, *375*, 65–73.  
 (15) Fleming, L.; Reynolds, N. *J. Chromatogr.* **1988**, *431*, 65–76.  
 (16) Reynolds, N. C.; Kissela, B. M.; Fleming, L. H. *Electroanalysis* **1995**, *7*, 1177–1181.  
 (17) Paras, C. D.; Kennedy, R. T. *Electroanalysis* **1997**, *9*, 203–208.  
 (18) Shen, H.; Lada, M. W.; Kennedy, R. T. *J. Chromatogr., B* **1997**, *704*, 43–52.  
 (19) Li, G. D.; Krull, I. S.; Cohen, S. A. *J. Chromatogr., A* **1996**, *724*, 147–157.  
 (20) Qu, Y.; Arckens, L.; Vandenbussche, E.; Geeraerts, S.; Vandesande, F. *J. Chromatogr., A* **1998**, *798*, 19–26.  
 (21) Luo, P. F.; Zhang, F. Z.; Baldwin, R. P. *Anal. Chim. Acta* **1991**, *244*, 169–178.  
 (22) Welch, L.; LaCourse, W.; Mead, D.; Johnson, D. *Anal. Chem.* **1989**, *61*, 555–559.  
 (23) Vanriel, J. A. M.; Olieman, C. *Anal. Chem.* **1995**, *67*, 3911–3915.  
 (24) Kok, W.; Hanekamp, H.; Bos, P.; Frei, R. *Anal. Chim. Acta* **1982**, *142*, 31–45.  
 (25) Kok, W.; Brinkman, U.; Frei, R. *J. Chromatogr.* **1983**, *256*, 17–26.  
 (26) Engstromsilverman, C. E.; Ewing, A. G. *J. Microcolumn Sep.* **1991**, *3*, 141–145.  
 (27) Stulik, K.; Pacakova, V.; Le, K.; Hennissen, B. *Talanta* **1988**, *35*, 455–460.  
 (28) Ye, J. N.; Baldwin, R. P. *Anal. Chem.* **1994**, *66*, 2669–2674.  
 (29) Luo, P. F.; Zhang, F. Z.; Baldwin, R. P. *Anal. Chem.* **1991**, *63*, 1702–1707.  
 (30) Luo, P. F.; Prabhu, S. V.; Baldwin, R. P. *Anal. Chem.* **1990**, *62*, 752–755.  
 (31) Kafil, J.; Huber, C. *Anal. Chim. Acta* **1985**, *175*, 275–280.  
 (32) Xie, Y. Q.; Huber, C. O. *Anal. Chem.* **1991**, *63*, 1714–1719.  
 (33) Prabhu, S.; Baldwin, R. *Anal. Chem.* **1989**, *61*, 852–856.  
 (34) Prabhu, S.; Baldwin, R. *Anal. Chem.* **1989**, *61*, 2258–2263.  
 (35) Colon, L. A.; Dadoo, R.; Zare, R. N. *Anal. Chem.* **1993**, *65*, 476–481.  
 (36) Tsai, H.; Weber, S. G. *Anal. Chem.* **1992**, *64*, 2897–2903.  
 (37) Chen, J. G.; Weber, S. G. *Anal. Chem.* **1995**, *67*, 3596–3604.  
 (38) Deacon, M.; Oshea, T. J.; Lunte, S. M.; Smyth, M. R. *J. Chromatogr., A* **1993**, *652*, 377–383.  
 (39) Singhal, P.; Kawagoe, K. T.; Christian, C. N.; Kuhr, W. G. *Anal. Chem.* **1997**, *69*, 1662–1668.  
 (40) Singhal, P.; Kuhr, W. G. *Anal. Chem.* **1997**, *69*, 3552–3557.  
 (41) Singhal, P.; Kuhr, W. G. *Anal. Chem.* **1997**, *69*, 4828–4832.  
 (42) Singhal, P.; Kuhr, W. G., submitted.

Thus, Fourier transformation of the time domain into the frequency domain allows the higher harmonics to be used to distinguish the faradiac signal from the major background components. As a result, the signal-to-noise ratio at the higher harmonics is increased and the sensitivity is improved. Long and Weber first used a large amplitude sine wave to simplify the process of Fourier transform digital filtering of voltammetric signals.<sup>43–45</sup> Unfortunately, the digital low-pass filter they implemented severely distorted the time domain signal once filtered, making it difficult to interpret the resulting voltammetry in the time domain.

In this work, we utilize the information in the frequency domain not only to improve the signal-to-noise ratio but also to gain selectively over different analytes. The “fingerprint” frequency domain response obtained for an analyte is hypothesized to be dependent on the kinetics of the oxidation reaction. The work presented here utilizes the advantages of SV to detect native amino acids, peptides, and a small protein at a copper microelectrode with flow injection analysis (FIA). The goal of this work is to create a universal detector that is both sensitive and selective toward amino acids, peptides, and small proteins.

## EXPERIMENTAL PARAMETERS

**Reagents.** The water used was deionized and then passed through a Milli-Q water purification system (Millipore Corp., Bedford, MA). The amino acids, insulin B-chain (98–99%, Sigma Chemical Corp., St. Louis, MO), and the remaining peptides (Peninsula Laboratories, Inc., San Carlos, CA) were all used as received. All experiments were performed with 0.10 M sodium hydroxide (ACS Grade, Fisher Scientific, Fair Lawn, NJ) as the running electrolyte. Stock solutions of 10 mM were made in deionized water, and subsequent dilutions were made using the running electrolyte.

**Copper Microelectrodes.** Copper microelectrodes were prepared by first pulling glass capillaries with a microelectrode puller (model PE-2, Narishige, Tokyo Japan). Then, under a microscope, the end of the capillary was clipped with a scalpel. A 25- $\mu$ m-diameter copper wire (99.99%, Goodfellow, Cambridge, England) was inserted into the freshly clipped end and sealed with epoxy (Resin 828, Miller-Stephenson Chemical Co., Inc., Danbury, CT). The exposed copper wire was cut flush against the glass capillary with a scalpel under a microscope. The electrode was then polished on a diamond polishing wheel and cleaned by sonication in deionized water. To make electrical connection with the copper wire, the capillary was back filled with gallium tin eutectic (Sigma Chemical Corp.) and a 150- $\mu$ m-diameter copper wire inserted into the gallium. Alternatively, electrical contact was made by back filling the capillary with epoxy and inserting the larger diameter copper wire until it made physical contact with the 25- $\mu$ m copper wire. The electrode was allowed to stabilize under experimental conditions for ~1 h or until a stable baseline was observed.

**Electrochemical Instrumentation and Experimental Conditions.** The FIA system has been described previously.<sup>39–41</sup> Briefly, the flow cell was constructed of plexiglass and designed so that the electrode is positioned 60 mm from the output of the

sample loop. The cell dimensions were designed to match the internal diameter of the FIA system’s tubing, 0.75 mm, to avoid broadening of the sample plug due to hydrodynamic mixing. The sample plug was injected with a pneumatic actuator (model 5701, Rheodyne, Cotati, CA) controlled by a solenoid valve (Rheodyne kit, model 7163). The flow rate was maintained through gravity flow by keeping the buffer reservoir 19 cm above the flow cell, resulting in a flow rate of 0.5 mL/min. To calculate the sample plug volume, the duration of the injection was multiplied by the flow rate. The injection time was chosen so that the electrode saw the full concentration of the analyte and was typically 30 s (0.250 mL) unless otherwise stated.

The excitation waveform used in this work was a digitally generated 2-Hz sine wave (0–690 mV vs Ag/AgCl) created with Labview software and applied with National Instruments hardware (PCI-4451, National Instruments, Austin, TX). The data acquisition card has 16-bit resolution with a maximum sampling rate of 200 kilosamples/s and was run using a 300-MHz Pentium II personal computer. The excitation waveform was filtered with a four-pole Bessel low-pass filter from a Cyberamp (model 380, Axon Instruments Inc., Foster City, CA) with a 3-dB point set at 3 times the fundamental frequency (6 Hz). The excitation was then applied to the electrochemical cell through a three-electrode potentiostat (Geneclamp 500, Axon Instruments Inc.). The current output was collected from the electrochemical cell, amplified by the potentiostat and filtered with a similar four-pole Bessel low-pass filter, 3-dB set at 80 Hz (4 times the maximum frequency collected, 10th harmonic or 20 Hz). The acquisition software was designed in house and collects 2 sinusoidal cycles, comprising 512 points, in a single scan and in real time continuously performs a fast Fourier transform. The scans are digitally sampled at 128 times the excitation frequency, 256 Hz, and ~300 scans are collected in a single experiment. The collection of a large number of points, on the order of 15 000, increases the resolution of the lower frequency components. Usually, only the first 10 harmonics of the frequency domain, consisting of a magnitude and phase angle for each, are saved to disk.

Postprocessing of the data was also performed with software written in-house utilizing a combination of Labview (National Instruments) and Matlab software (The Mathworks, Inc., Englewood Cliffs, NJ). Frequency domain information is obtained through a data reduction process that has been described previously.<sup>39</sup> Briefly, the current response can be thought of as a series of instantaneous current vectors, which occur at the fundamental frequency, and odd and even harmonics. Prior to injection, each current vector is composed solely of the background current,  $\bar{B}$ , which typically has a fixed magnitude and phase angle. When the analyte is injected, the instantaneous current vector changes to include both signal and background components ( $\bar{S} + \bar{B}$ ). First, the background component,  $\bar{B}$ , at each harmonic is digitally subtracted from the entire data set to give the signal only vector,  $\bar{S}$ . The frequency domain information for the analyte signal is obtained from the time point at each harmonic in the FIA time course where the magnitude is at a maximum.

In addition to the frequency domain information, time course data can be obtained for each frequency element.<sup>39</sup> A “digital equivalent” of a lock-in amplifier is applied to the time course data. Briefly, the instantaneous vector ( $\bar{I}$ ) is projected onto the signal

(43) Weber, S. G.; Long, J. T. *Anal. Chem.* **1988**, *60*, 903A–913A.

(44) Reich, G.; Wolf, J.; Long, J. T.; Weber, S. G. *Anal. Chem.* **1990**, *62*, 2643–2646.

(45) Long, J. T.; Weber, S. G. *Electroanalysis* **1992**, *4*, 429–437.

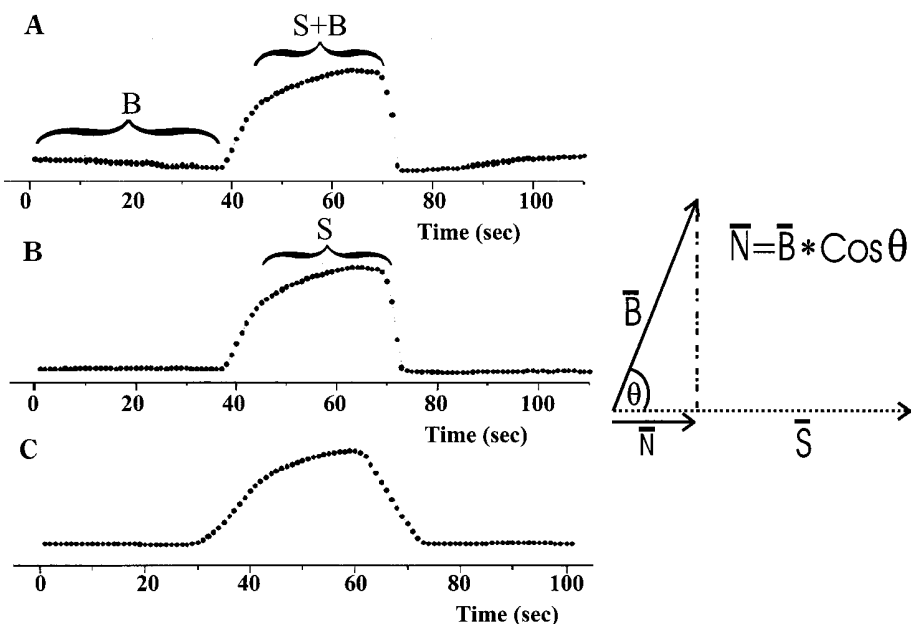


Figure 1. Noise reduction using a digital lock-in amplifier. (A) The raw time course data for an analyte at a certain harmonic. (B) The same time course data shown in (A) after phase optimization. (C) A low-pass filter (boxcar average) is applied to the phase-optimized time course in (B) as the final step in the digital lock-in process.

vector ( $\bar{S}$ ). Thus, the instantaneous current is monitored at the phase angle of the signal, consequently only the background component at that angle is observed while the rest is eliminated. The most dramatic elimination of background occurs when the difference in phase angle of the signal and background is  $90^\circ$ . The final step is to low-pass filter the phase-optimized time course data with a boxcar averaging routine.

## RESULTS AND DISCUSSION

Copper electrodes have been used extensively to detect native aliphatic molecules. Carbohydrates,<sup>33–35</sup> nucleotides,<sup>40</sup> ds- and ss-DNA,<sup>41,42</sup> amino acids, and peptides<sup>24–29</sup> are among the most common classes of molecules that have been detected at copper. Two primary mechanisms of detection have been proposed. The first mechanism, involving the complexation of the analyte with Cu(II) on the surface of the electrode, is not applicable to larger peptides and small proteins.<sup>28</sup> The second mechanism, involving an electrocatalytic reaction, is more likely to represent the mode of detection employed herein to study native amino acids and larger peptides. This catalytic mechanism is complex in nature and involves a hydroxide/oxide layer that forms on the electrode surface in alkaline solutions.<sup>28,33–35</sup> Under these conditions, Ye and Baldwin used cyclic voltammetry to show that the oxidation of all amino acids produces an increase in anodic current between 0.4 and 0.8 V vs Ag/AgCl.<sup>28</sup> This potential region is near or superimposed onto the Cu(II)/Cu(III) redox couple wave. For this reason, many investigators have hypothesized that the Cu(III) species participates in the catalytic oxidation of these analytes.<sup>28,33–35</sup> This conclusion is verified further by the observation that the anodic Cu(II)/Cu(III) redox wave is present on the first scan of a copper electrode but disappears as it is scanned further.<sup>35</sup> When the electrode is exposed to the analyte, the anodic Cu(II)/Cu(III) redox wave reappears, indicating that the Cu(III) species in the outer layer of the copper electrode catalytically oxidizes the analyte and is converted back into the Cu(II) species.

The use of a sine wave enables the discrimination between background and faradaic processes in the frequency domain, specifically at the higher harmonics.<sup>43,45</sup> The discrimination between signal and noise in SV is enhanced further through the application of a software lock-in amplifier on the time course data. The signal component can be isolated from the instantaneous current by locking onto the signal's phase angle.<sup>39</sup> The resulting phase-locked component is plotted as a function of time to create a time course profile in an FIA experiment. The extent of noise reduction is determined by the angle separating the signal from the background vector, such that the most dramatic minimization in rms noise occurs when this angle is close to  $90^\circ$ .

Figure 1 illustrates the steps involved in phase optimization of the time course data. The first trace, Figure 1A, is the raw magnitude collected at the fourth harmonic (8 Hz). This is merely the FFT magnitude at the fourth harmonic plotted as a function of time. The initial rms noise, without any additional software processing, is quite large (3.8 pA). Figure 1B represents the time course data after locking in and monitoring only at the signal's phase angle ( $85^\circ$ ). The improvement in rms noise is almost 1 order of magnitude (shown in Figure 1B). The final time course represented in Figure 1C is the final application of a 10-point boxcar average. The total improvement in rms noise in this case is over 1 order of magnitude from raw data to the final step in the data processing. Typically, examining all the harmonics and finding the one with the highest S/N level determines the best LOD for a particular analyte. Implementation of the digital lock-in in software allows the examination of all the frequency components of the signal simultaneously, greatly simplifying the selection of the optimized signal frequency and phase angle. With its narrow bandwidth, phase-resolved SV can attain or even surpass the sensitivity of dc amperometry, while maintaining the selectivity of a scanning technique.

One of the main drawbacks of dc amperometry at a copper electrode is that there is an inherent lack of selectivity between molecules, since the oxidation reaction depends on the same electrocatalytic mechanism. The voltammetry of the oxidation of most aliphatic molecules is indistinguishable.<sup>28</sup> Therefore, a separation step is required to discriminate between different analytes. With SV, additional selectivity is obtained in the frequency domain spectrum of each analyte. A unique "fingerprint" frequency domain spectrum can be obtained for each analyte, and the magnitude and phase angle of each frequency element depends on a variety of parameters, including electron-transfer kinetics.<sup>39–41</sup> This frequency domain spectrum is obtained by digitally subtracting the background vector from the entire data set to isolate the signal (see Experimental Parameters for details). When this is combined with an electrocatalytic mechanism (i.e., at Cu), this allows the detection of a wide variety of amino acids, including those that are not electroactive at conventional electrode materials.

The SV frequency spectra for a variety of amino acids, arginine (Arg), asparagine (Asn), and glutamine (Gln), are shown in Figure 2. Figure 2A is a 1  $\mu$ M FIA injection of Arg with the first 10 harmonics collected and displayed (2–20 Hz). The frequency spectrum shown is unique to the electrocatalytic oxidation kinetics of Arg at copper. The SV frequency spectrum contains three pieces of information; the frequency of the harmonic (Hz), the magnitude (nA), and the phase angle (degrees) of the current measured at each harmonic. The magnitude of the current at each frequency component is proportional to the concentration of the analyte. The detection of 1  $\mu$ M arginine gave reproducible current responses with a standard deviation of  $\pm 15$  pA ( $n = 5$ , two different electrodes) at the third harmonic. The phase angle at each frequency component is unique to the analyte and independent of the concentration injected. The phase angles remain consistent from run to run with an average deviation of  $\pm 10^\circ$ . For example, with repetitive injections of arginine, the phase angle at the third harmonic has a standard deviation of  $\pm 8.2^\circ$  ( $n = 5$ , two different electrodes). Thus, the phase angle information depicted in Figure 2A is specific for the oxidation of Arg at a copper electrode and can be used to selectively identify it.

The overlaid plots in Figure 2B are the frequency responses of Asp and Gln obtained under identical conditions. These amino acids are structurally similar to one another, differing only by one methylene group in the side chain. As might be expected, the frequency spectra of the two amino acids in Figure 2B are similar up to the fourth harmonic. However, the two spectra deviate at higher harmonics. Closer examination of the signal at the fifth harmonic (10 Hz) indicates that the phase angles differ by  $120^\circ$ , presumably due to differences in the kinetics of oxidation at Cu.

The phase-optimized time course for the third harmonic (6 Hz) of a 1  $\mu$ M injection of Arg is shown in Figure 3. This harmonic has the greatest signal-to-noise ratio for the oxidation of arginine and best phase optimization ( $\Delta\phi = 76^\circ$ ), resulting in a LOD (S/N = 3) of 35 nM (roughly 4-fold lower than achieved with dc amperometry).<sup>29</sup> The time course data also show the signal returns to the background level immediately after the injection, indicating the absence of adsorption processes at the electrode. The use of a large-amplitude sine wave results in continuous oxidation and reduction of the copper surface, which cleans and retains the

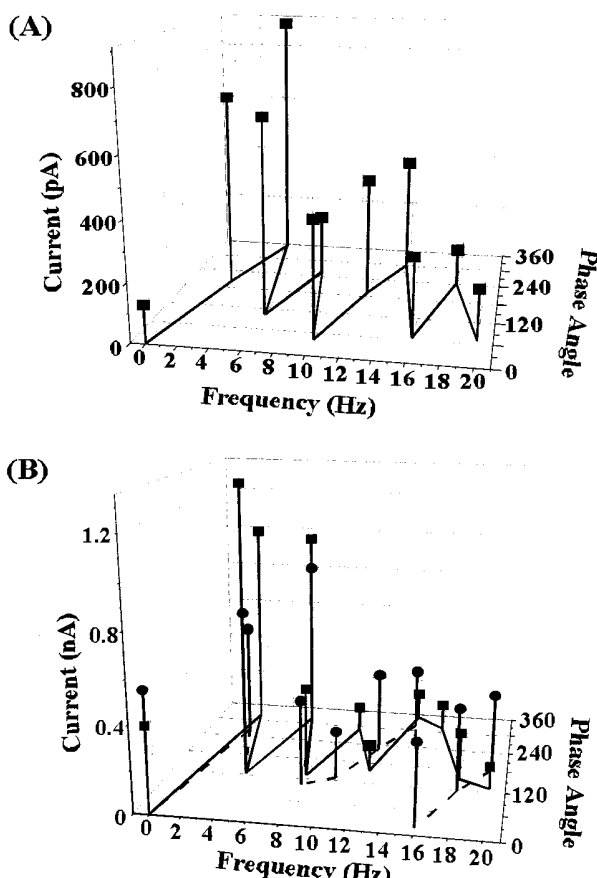


Figure 2. Background-subtracted frequency spectrum for arginine, asparagine, and glutamine. (A) The background-subtracted frequency response of a 1  $\mu$ M FIA injection of arginine. (B) The background-subtracted frequency responses of 10  $\mu$ M injections of asparagine (circles) and glutamine (squares). The excitation in both spectra is a 2-Hz sine wave, 0–690 mV vs Ag/AgCl. The running electrolyte used was 0.10 M NaOH. Current from two sinusoidal periods, consisting of 512 points (total time, 1 s), were used to generate each frequency spectrum. The three-dimensional graph contains three pieces of information: the frequency (x-axis), magnitude (z-axis), and phase angle (y-axis) of the first 10 harmonics.

activity of the electrode. The maintenance of a clean and active copper surface allows a single electrode to be used for two weeks or more with minimal signal degradation.

The response of the system was then examined for the neurologically active peptides, luteinizing hormone-releasing hormone (LHRH), bradykinin, neurotensin, and substance P, to determine the sensitivity and selectivity for larger molecules. The amino acid content of each of these peptides is shown in Table 1. Bradykinin and LHRH both contain 9 amino acid residues, whereas neurotensin and substance P contain 13 and 11 amino acid residues, respectively. The frequency responses for LHRH and bradykinin are overlaid and shown in Figure 4A. As can be seen from these spectra, the two peptides are dramatically different in their response, presumably because of differing rates of electrocatalytic oxidation at the copper electrode.

The frequency spectra of the larger peptides, neurotensin and substance P, are shown in Figure 4B. These two peptides have similar frequency responses implying similar oxidation kinetics at copper. The signal intensity for both peptides falls off dramati-

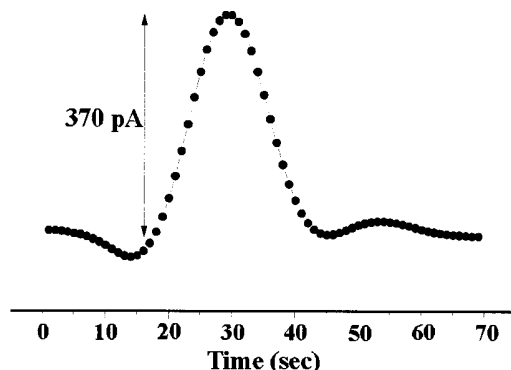


Figure 3. Time course of  $1 \mu\text{M}$  arginine at the third harmonic (6 Hz) from the same injection shown in Figure 2A. The harmonic shown, third, gives the greatest signal-to-noise ratio, with a LOD (S/N = 3) of  $35 \text{ nM}$ .

Table 1

peptide	amino acid content
luteinizing hormone-releasing hormone	pGlu-His-Trp-Ser-Gly-Leu-Arg-Pro-Gly-NH <sub>2</sub>
bradykinin	Arg-Pro-Pro-Gly-Phe-Ser-Pro-Phe-Arg
neurotensin	pGlu-Leu-Tyr-Glu-Asn-Lys-Pro-Arg Arg-Pro-Tyr-Ile-Leu
substance P	Arg-Pro-Lys-Pro-Gln-Gln-Phe-Phe-Gly-Leu-Met-NH <sub>2</sub>

cally after the fifth harmonic (data not shown). The most likely reason that the current magnitude is diminished at higher harmonics is probably due to slower oxidation kinetics of the larger peptides, limiting the signal to the lower order harmonics. A slower sine wave excitation could be used to increase the number of harmonics containing observable signal and help differentiate the frequency domain spectra for the two peptides, but that was not investigated in this work.

Time course data for each of the four peptides studied are shown in Figure 5. Figure 5A represents the injection of a  $10 \mu\text{M}$  sample of the two larger peptides, neurotensin and substance P, as measured at the first harmonic (2 Hz). From these data, the calculated limit of detection for neurotensin and substance P are  $15$  and  $40 \text{ nM}$ , respectively. This LOD is over 1 order of magnitude better than peptides of similar size or smaller reported for electrocatalytic detection at a copper electrode.<sup>28,29</sup> The time course data for LHRH and bradykinin observed at the fourth harmonic (8 Hz) are shown in Figure 5B with calculated LOD of  $66$  and  $10 \text{ nM}$ , respectively. This seems to indicate that SV detection used in conjunction with an electrocatalytic mechanism can lead to extremely good sensitivity for a wide variety of peptides, regardless of their amino acid composition.

A phase-locked signal can also be used to reduce or eliminate interferences in the sample matrix. For example, the optimized signal phase angles for LHRH and bradykinin differ by  $66^\circ$  at the fourth harmonic. The time course traces in Figure 5B illustrates how well this system works at rejecting unwanted signals. In the first panel, the optimized signal for LHRH signal observed at the fourth harmonic (solid line with circles) is superimposed over a time course for bradykinin (dotted line with squares) at the same phase angle ( $70^\circ$ ). By phase-locking the signal at  $70^\circ$ , most of the bradykinin signal is eliminated. In the second panel, the same

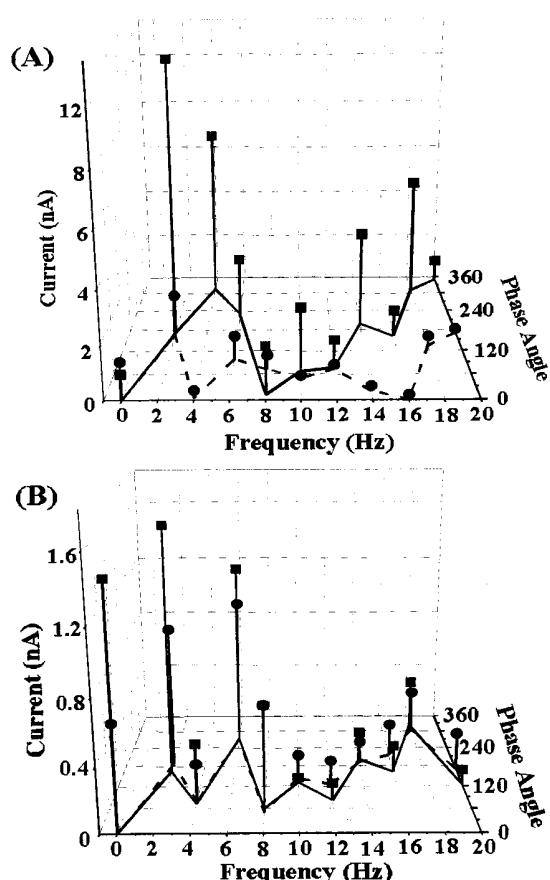


Figure 4. Subtracted frequency spectra of the neuroactive peptides. (A) The subtracted frequency responses for  $10 \mu\text{M}$  injections of luteinizing hormone-releasing hormone (circles) and bradykinin (squares) in FIA. (B) The subtracted frequency responses for  $10 \mu\text{M}$  injections of substance P (circles) and neurotensin (squares) under identical conditions. The experimental conditions are the same as in Figure 2.

procedure was followed for the isolation of the bradykinin signal (solid line with square symbols) observed at its optimum phase angle ( $4^\circ$ ), superimposed over a time course for LHRH (dotted line with circles) at the same phase angle. The signal for each of the peptides is effectively reduced at the "wrong" phase angle, where the signal for the desired peptide was optimized. Thus, interferences can be minimized by monitoring at the harmonic where the analyte and interference are closest to  $90^\circ$  out of phase. This would be especially attractive for measurements *in vivo*, where the sample matrix is complex and contains potential interferences. This work is being pursued further in our laboratory to determine whether a signal can be measured in a complex mixture of electroactive interferences.

Insulin B-chain is an important small protein that contains  $30$  amino acid residues. This molecule was chosen to determine the applicability of this detection approach for a significantly larger molecule. Kennedy et al. have done extensive work on the detection of insulin.<sup>46,47</sup> They used a carbon electrode modified

(46) Aspinwall, C. A.; Lakey, J. R. T.; Kennedy, R. T. *J. Biol. Chem.* **1999**, *274*, 6360–6365.

(47) Aspinwall, C. A.; Brooks, S. A.; Kennedy, R. T.; Lakey, J. R. T. *J. Biol. Chem.* **1997**, *272*, 31308–31314.

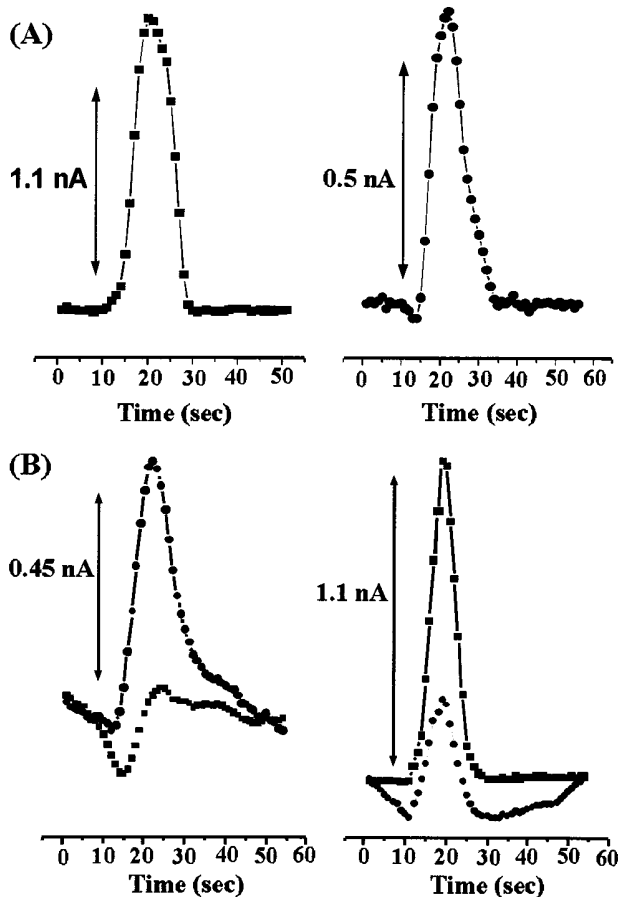


Figure 5. Time course for FIA of neuroactive peptides. (A) Time course data for the FIA injections in Figure 4B of neurotensin (left, squares) and substance P (right, circles). The time course data shown are at the first harmonic (2 Hz) and give LOD for neurotensin and substance P ( $S/N = 3$ ) of 15 and 40 nM, respectively. (B) Time course data for the injections in Figure 4A of LHRH (left, circles) and bradykinin (right, squares). The solid line is the phase-optimized time course at the fourth harmonic (8 Hz) for each analyte. The LOD for LHRH and bradykinin ( $S/N = 3$ ) at this harmonic are 66 and 10 nM, respectively. The dotted, less intense traces are the time course data for each peptide using the optimized phase angle of the other. The experimental conditions are the same as in Figure 2.

with a mixed valent film of cyanoruthenate and ruthenium oxide to characterize the release of insulin from pancreatic cells *in vivo*. Figure 6 shows the frequency and time course data for a 10  $\mu$ M injection of insulin B-chain. Again, there is signal present only out to the fourth harmonic (8 Hz), due to the slower reaction kinetics of this large molecule. The time course data at the third harmonic (6 Hz) gives the best  $S/N$  ratio with a detection limit of 200 nM ( $S/N = 3$ ). The detection limit is limited by the size and slower electron-transfer kinetics of this molecule. The optimization of the excitation frequency was not pursued in this work, but presumably lower excitation frequency could be used to enhance the detection limit.

## CONCLUSIONS

SV at a copper electrode is a sensitive and selective technique for the detection of amino acids, peptides, and small proteins. The ability to detect these molecules in their native state eliminates

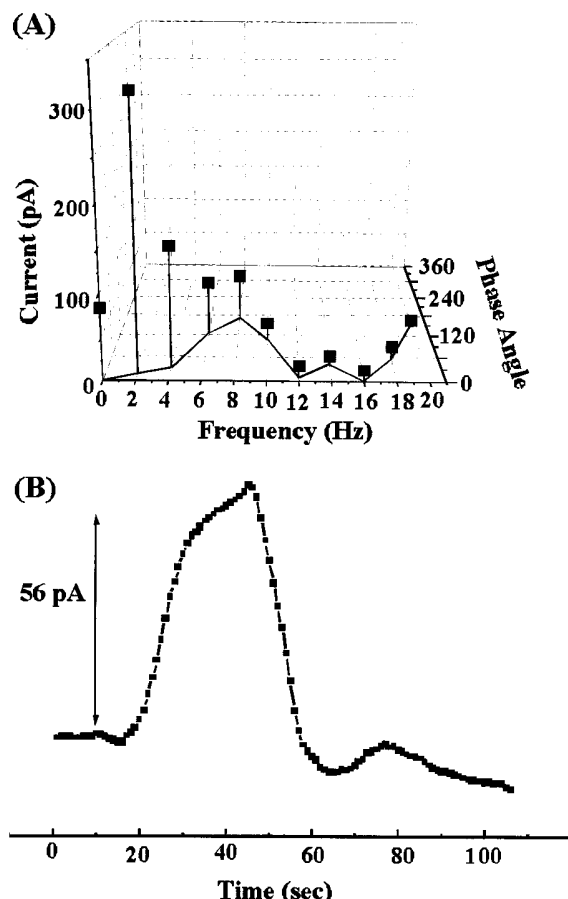


Figure 6. Frequency spectrum and time course data for FIA of insulin B-chain. (A) The optimized frequency spectrum for a 10  $\mu$ M injection of insulin B-chain. (B) The time course data at the third harmonic (6 Hz) for the injection in (A). The LOD ( $S/N = 3$ ) for this harmonic is 200 nM. The same experimental conditions as in Figure 2 were used.

the need for derivatization steps. The sensitivity obtained for the molecules studied is roughly 4–10-fold better than reported for dc amperometric detection at copper. SV also possesses the selectivity of a voltammetric technique, in that the information gained in the frequency domain is analyte specific. Interferences can be minimized by phase locking the signal at phase angles where the interference signal is minimized, effectively nulling out potential background interferences. This is an attractive advantage for detecting analytes in complex matrixes. SV is also easily coupled to HPLC, CE, and other separation techniques because it is fast, sensitive, and selective (allowing three-dimensional data for all analytes detected) and electrode fouling is less of a problem.

## ACKNOWLEDGMENT

This work was supported by the National Institutes of Health (Grant 1R21HG01828-01).

Received for review May 11, 2000. Accepted August 31, 2000.

AC000543R